

# The $B_c \rightarrow \psi(2S)\pi, \eta_c(2S)\pi$ decays in the perturbative QCD approach

Zhou Rui<sup>1,\*</sup>, Wen-Fei Wang<sup>2,3</sup>, Guang-xin Wang<sup>1</sup>, Li-hua Song<sup>1</sup>, and Cai-Dian Lü<sup>3</sup>

<sup>1</sup>*College of Sciences, North China University of Science and Technology, Tangshan 063009, China,*

<sup>2</sup>*Department of Physics and Institute of Theoretical Physics,  
Shanxi University, Taiyuan, Shanxi 030006, China,*

<sup>3</sup>*Center for Future High Energy Physics, Institute of High Energy Physics,  
Chinese Academy of Sciences, Beijing 100049, China*

(Dated: June 10, 2019)

Nonleptonic two body  $B_c$  decays including radially excited  $\psi(2S)$  or  $\eta_c(2S)$  mesons in the final state are studied using the perturbative QCD approach based on  $k_T$  factorization. The charmonium distribution amplitudes are extracted from the  $n = 2, l = 0$  Schrödinger states for the harmonic oscillator potential. Utilizing these distribution amplitudes, we calculate the numerical results of the  $B_c \rightarrow \psi(2S), \eta_c(2S)$  transition form factors and branching fractions of  $B_c \rightarrow \psi(2S)\pi, \eta_c(2S)\pi$  decays. The ratio between two decay modes  $B_c \rightarrow \psi(2S)\pi$  and  $B_c \rightarrow J/\psi\pi$  is compatible with the experimental data within uncertainties, which indicate that the harmonic oscillator wave functions for  $\psi(2S)$  and  $\eta_c(2S)$  work well. It is found that the branching fraction of  $B_c \rightarrow \eta_c(2S)\pi$ , which is dominated by the twist-3 charmonium distribution amplitude, can reach the order of  $10^{-3}$ . We hope it can be measured soon in the LHCb experiment.

PACS numbers: 13.25.Hw, 12.38.Bx, 14.40.Nd

## I. INTRODUCTION

The meson  $B_c$ , a pseudoscalar ground state of  $b$  and  $c$  quarks, can only decay through weak interactions. Either of the heavy quarks ( $b$  or  $c$ ) in it can decay individually, which makes it an ideal system to study weak decays of heavy quarks. Around  $\mathcal{O}(10^9)$  mesons can be anticipated with  $1 \text{ fb}^{-1}$  of data at the LHC [1], which is sufficient for studying the  $B_c$  meson family systematically. Up to now, several new decay channels of the  $B_c$  meson [2–6] have been successfully observed by the LHCb Collaboration; While an excited  $B_c$  meson state which is consistent with expectations of the  $B_c(2S)$  has been caught by the ATLAS detector [7].

Recently, the LHCb Collaboration observed the decay mode  $B_c \rightarrow \psi(2S)\pi$  for the first time with the measured ratio of the branching fractions as [8]

$$\frac{\mathcal{B}(B_c \rightarrow \psi(2S)\pi)}{\mathcal{B}(B_c \rightarrow J/\psi\pi)} = 0.250 \pm 0.068(\text{stat}) \pm 0.014(\text{syst}) \pm 0.006(\mathcal{B}). \quad (1)$$

The last term above accounts for the uncertainty on  $\mathcal{B}(\psi(2S) \rightarrow \mu^+\mu^-)/\mathcal{B}(J/\psi \rightarrow \mu^+\mu^-)$ . Although there is not much data for the  $B_c$  meson decaying into two-body final states containing a radially excited charmonium such as  $\psi(2S)$  or  $\eta_c(2S)$  except  $B_c \rightarrow \psi(2S)\pi$  channel, many theoretical studies of nonleptonic  $B_c$  decays with radially excited charmonium mesons in final state have been performed by using various approaches. For example, in Ref. [9], the authors computed the branching ratios for  $B_c \rightarrow \psi(2S)X$  decays with the modified harmonic oscillator wave function in the light front quark model; in Ref. [10], the ISGW2 quark model was adopted to study the production of radially excited charmonium mesons in two-body nonleptonic  $B_c$  decays; while the relativistic (constituent) quark model, the potential model, the QCD relativistic potential model and the improved instantaneous BS equation and Mandelstam approach were adopted in Refs. [11, 12], Ref. [13], Ref [14] and Ref [15], respectively. However, all of these calculations are based on a naive factorization hypothesis, with various form factor inputs. There are uncontrolled large theoretical errors with quite different numerical results, and most of them can not give any theoretical error estimates because of the nonreliability of these models.

The perturbative QCD approach (pQCD) [16] based on  $k_T$  factorization, which not only can deal with the emission diagrams corresponding to the naive factorization terms basically, but can also handle well the nonfactorizable diagrams by introducing the wave function of the light meson in the final states of the  $B_c$  decay modes, is widely used in the nonleptonic two-body  $B_c$  decays [17–28]. In our recent work [29], the pQCD approach was used successfully in

---

\*Electronic address: zhourui@ncst.edu.cn

describing the S-wave ground state charmonium decays of  $B_c$  meson based on the harmonic-oscillator wave functions for the charmonium 1S states. In this work, we will use the harmonic oscillator wave function as the approximate wave function of the 2S states, and study the  $B_c \rightarrow \psi(2S)\pi, \eta_c(2S)\pi$  decays in the pQCD approach to provide a ready reference to the existing and forthcoming experiments.

The structure of this paper is organized as follows. After this Introduction, we describe the wave functions of radially excited charmonium mesons  $\psi(2S), \eta_c(2S)$  in Sec. II. We calculate and present the expressions for the  $B_c \rightarrow \psi(2S), \eta_c(2S)$  transition form factors in the large recoil regions and the  $B_c \rightarrow \psi(2S)\pi, \eta_c(2S)\pi$  decay amplitudes in Sec. III. The numerical results and relevant discussions are given in Sec. IV, and Sec. V contains a brief summary.

## II. WAVE FUNCTIONS

In hadronic B decays, there are several energy scales involved. In the expansion of the inverse power of heavy quark mass, the hadronic matrix element can be factorized into perturbative and non-perturbative factors. In the pQCD approach, the decay amplitude  $\mathcal{A}(B_c \rightarrow M_2 M_3)$  can be written conceptually as the convolution [16],

$$\mathcal{A}(B_c \rightarrow M_2 M_3) \sim \int d^4 k_1 d^4 k_2 d^4 k_3 \text{Tr} [C(t)\Phi_{B_c}(k_1)\Phi_{M_2}(k_2)\Phi_{M_3}(k_3)H(k_1, k_2, k_3, t)], \quad (2)$$

where  $k_i$ 's are momenta of spectator quarks included in each meson, and ‘‘Tr’’ denotes the trace over Dirac and color indices. In the above convolution,  $C(t)$  is the Wilson coefficient evaluated at scale  $t$ , the function  $H(k_1, k_2, k_3, t)$  describes the four quark operator and the spectator quark connected by a hard gluon, which can be perturbatively calculated including all possible Feynman diagrams without end-point singularity. The wave function  $\Phi_{B_c}(k_1)$ ,  $\Phi_{M_2}$  and  $\Phi_{M_3}$  describe the hadronization of the quark and anti-quark in the  $B_c$  meson, the charmonium meson  $\psi(2S)$  or  $\eta_c(2S)$  and the final state light meson pion, respectively.

As a heavy quarkonium discussed in Refs. [29, 30], the nonrelativistic QCD framework can be applied for the  $B_c$  meson, which means its leading-order wave function should be just the zero-point wave function with the distribution amplitude

$$\phi_{B_c}(x) = \frac{f_{B_c}}{2\sqrt{2N_c}} \delta(x - m_c/m_{B_c}) \exp[-\omega_{B_c}^2 b^2/2]. \quad (3)$$

For the light meson pion, we adopt the same distribution amplitudes  $\phi_\pi^A(x)$  and  $\phi_\pi^{P,T}(x)$  as defined in Refs. [31, 32].

The harmonic oscillator wave functions has been adopted to describe the 1S state mesons [33–35], and they can explain the experimental data well [29]. In the quark model,  $\eta_c(2S)$  and  $\psi(2S)$  are the first excited states of  $\eta_c$  and  $J/\psi$ , respectively. The 2S means that for these states, the principal quantum number  $n = 2$  and the orbital angular momentum  $l = 0$ . The definition of the 2S state wave functions are similar with the 1S states via the nonlocal matrix elements [36],

$$\begin{aligned} \langle \psi(2S)(P, \epsilon^L) | \bar{c}(z)_\alpha c(0)_\beta | 0 \rangle &= \frac{1}{\sqrt{2N_c}} \int_0^1 dx e^{ixP \cdot z} [m \not{\epsilon}^L_{\alpha\beta} \psi^L(x, b) + (\not{\epsilon}^L P)_{\alpha\beta} \psi^t(x, b)], \\ \langle \psi(2S)(P, \epsilon^T) | \bar{c}(z)_\alpha c(0)_\beta | 0 \rangle &= \frac{1}{\sqrt{2N_c}} \int_0^1 dx e^{ixP \cdot z} [m \not{\epsilon}^T_{\alpha\beta} \psi^V(x, b) + (\not{\epsilon}^T P)_{\alpha\beta} \psi^T(x, b)], \\ \langle \eta_c(2S)(P) | \bar{c}(z)_\alpha c(0)_\beta | 0 \rangle &= -\frac{i}{\sqrt{2N_c}} \int_0^1 dx e^{ixP \cdot z} [(\gamma_5 P)_{\alpha\beta} \psi^v(x, b) + m(\gamma_5)_{\alpha\beta} \psi^s(x, b)], \end{aligned} \quad (4)$$

where  $P$  stands for the momentum of the charmonium meson  $\eta_c(2S)$  or  $\psi(2S)$  and  $m$  is its mass. The  $x$  represents the momentum fraction of the charm quark inside the charmonium, and  $b$  is the conjugate variable of the transverse momentum of the valence quark of the meson. The  $\epsilon^{L(T)}$  denotes its longitudinal (transverse) polarization vector. The asymptotic models for the twist-2 distribution amplitudes  $\psi^{L,T,v}$ , and the twist-3 distribution amplitudes  $\psi^{t,V,s}$  will be derived following the prescription in [33].

First, we write down the Schrödinger equal-time wave function  $\Psi_{Sch}(\mathbf{r})$  for the harmonic oscillator potential. The radial wave function of the corresponding Schrödinger state is given by

$$\Psi_{(2S)}(\mathbf{r}) \propto \left(\frac{3}{2} - \alpha^2 r^2\right) e^{-\frac{\alpha^2 r^2}{2}}, \quad (5)$$

where  $\alpha^2 = \frac{m\omega}{2}$  and  $\omega$  is the frequency of oscillations or the quantum of energy. Then we perform the Fourier transformation to the momentum space to get  $\Psi_{2S}(\mathbf{k})$  as

$$\Psi_{(2S)}(\mathbf{k}) \propto (2k^2 - 3\alpha^2) e^{-\frac{k^2}{2\alpha^2}}, \quad (6)$$

with  $k^2$  being the square of three momentum. In terms of the substitution assumption

$$\mathbf{k}_\perp \rightarrow \mathbf{k}_\perp, \quad k_z \rightarrow \frac{m_0}{2}(x - \bar{x}), \quad m_0^2 = \frac{m_c^2 + \mathbf{k}_\perp^2}{x\bar{x}}, \quad (7)$$

with  $m_c$  the  $c$ -quark mass and  $\bar{x} = 1 - x$ . We should make the following replacement towards the variable  $k^2$

$$k^2 \rightarrow \frac{\mathbf{k}_\perp^2 + (x - \bar{x})^2 m_c^2}{4x\bar{x}}. \quad (8)$$

Then, the wave function can be taken as

$$\Psi_{(2S)}(\mathbf{k}) \rightarrow \Psi_{(2S)}(x, \mathbf{k}_\perp) \propto \left( \frac{\mathbf{k}_\perp^2 + m_c^2(x - \bar{x})^2}{2x\bar{x}} - 3\alpha^2 \right) e^{-\frac{\mathbf{k}_\perp^2 + m_c^2(x - \bar{x})^2}{8x\bar{x}\alpha^2}}. \quad (9)$$

Applying the Fourier transform to replace the transverse momentum  $\mathbf{k}_\perp$  with its conjugate variable  $b$ , the 2S oscillator wave function can be taken as

$$\begin{aligned} \Psi_{(2S)}(x, \mathbf{b}) &\sim \int d^2\mathbf{k}_\perp e^{-i\mathbf{k}_\perp \cdot \mathbf{b}} \Psi_{(2S)}(x, \mathbf{k}_\perp) \\ &\propto x\bar{x} \mathcal{T}(x) e^{-x\bar{x} \frac{m_c}{\omega} [\omega^2 b^2 + (\frac{x-\bar{x}}{2x\bar{x}})^2]}, \end{aligned} \quad (10)$$

with

$$\mathcal{T}(x) = 1 - 4b^2 m_c \omega x \bar{x} + \frac{m_c(x - \bar{x})^2}{\omega x \bar{x}}. \quad (11)$$

We then propose the 2S states distribution amplitudes inferred from Eq. (10),

$$\Psi_{(2S)}(x, b) \propto \Phi^{asy}(x) \mathcal{T}(x) e^{-x\bar{x} \frac{m_c}{\omega} [\omega^2 b^2 + (\frac{x-\bar{x}}{2x\bar{x}})^2]}, \quad (12)$$

with the  $\Phi^{asy}(x)$  being the asymptotic models, which have been given in [37]. Therefore, we have the distribution amplitudes for the radially excited charmonium mesons  $\eta_c(2S)$  and  $\psi(2S)$

$$\begin{aligned} \Psi^{L,T,v}(x, b) &= \frac{f_{2S}}{2\sqrt{2N_c}} N^{L,T,v} x\bar{x} \mathcal{T}(x) e^{-x\bar{x} \frac{m_c}{\omega} [\omega^2 b^2 + (\frac{x-\bar{x}}{2x\bar{x}})^2]}, \\ \Psi^t(x, b) &= \frac{f_{2S}}{2\sqrt{2N_c}} N^t (x - \bar{x})^2 \mathcal{T}(x) e^{-x\bar{x} \frac{m_c}{\omega} [\omega^2 b^2 + (\frac{x-\bar{x}}{2x\bar{x}})^2]}, \\ \Psi^V(x, b) &= \frac{f_{2S}}{2\sqrt{2N_c}} N^V [1 + (x - \bar{x})^2] \mathcal{T}(x) e^{-x\bar{x} \frac{m_c}{\omega} [\omega^2 b^2 + (\frac{x-\bar{x}}{2x\bar{x}})^2]}, \\ \Psi^s(x, b) &= \frac{f_{2S}}{2\sqrt{2N_c}} N^s \mathcal{T}(x) e^{-x\bar{x} \frac{m_c}{\omega} [\omega^2 b^2 + (\frac{x-\bar{x}}{2x\bar{x}})^2]}, \end{aligned} \quad (13)$$

with the normalization conditions:

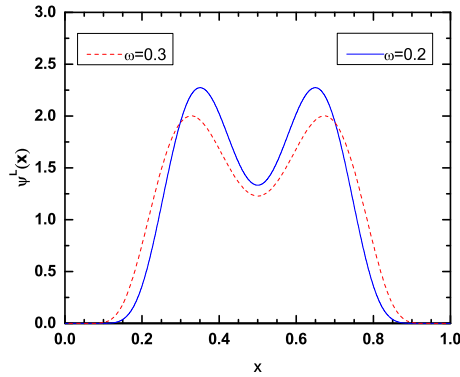


FIG. 1: The shape of the distribution amplitude for  $\psi^L(x)$  when  $b = 0$ , with the solid (dashed) line for  $\omega = 0.2(0.3)$  GeV.

$$\int_0^1 \Psi^i(x, 0) dx = \frac{f_{2S}}{2\sqrt{2N_c}}. \quad (14)$$

The  $N_c$  above is the color number,  $N^i (i = L, T, t, V, v, s)$  are the normalization constants, and  $f_{2S}$  is the decay constant of 2S state. All the distribution amplitudes in Eq. (13) are symmetric under  $x \leftrightarrow \bar{x}$ . Here we do not distinguish the leading twist distribution amplitude  $\Psi^v$  of the  $\eta_c(2S)$  meson from  $\Psi^{L,T}$  of the  $\psi(2S)$  meson, and the same decay constant has been assumed for the longitudinally and transversely polarized  $\psi(2S)$  meson. To be more clear, the shape of the distribution amplitude  $\Psi^L(x, 0)$  is displayed in Fig. 1. The free parameter  $\omega = 0.2$  GeV is adopt, such that the valence charm quark, carrying the invariant mass  $x^2 P^2 \approx m_c^2$ , is almost on shell. It can be seen that the two maximum positions are near  $x = 0.35$  and  $x = 0.65$  and a larger value of parameter  $\omega$  gives a wider shape. Note that the dip at  $x = 0.5$  is a consequence of the radial Schrödinger wave function of  $n = 2, l = 0$  state.

### III. FORM FACTORS AND DECAY AMPLITUDES

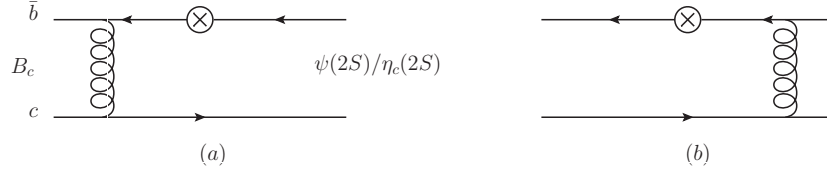


FIG. 2: The leading order Feynman diagrams for the  $B_c \rightarrow (\psi(2S), \eta_c(2S))$  transitions.

In pQCD approach, the  $B_c \rightarrow \psi(2S), \eta_c(2S)$  transition form factors at large recoil limit ( $q^2 = 0$ ), which are similar to that of  $B_c \rightarrow J/\psi, \eta_c$  [38], can be calculated from above universal hadronic distribution amplitudes. The lowest order diagrams are displayed in Fig. 2. The form factors  $F_{+,0}(q^2)$ ,  $V(q^2)$  and  $A_{0,1,2}(q^2)$  are defined via the matrix element [39],

$$\langle \eta_c(2S)(P_2) | \bar{c} \gamma^\mu b | B_c(P_1) \rangle = \left[ (P_1 + P_2)^\mu - \frac{M^2 - m^2}{q^2} q^\mu \right] F_+(q^2) + \frac{M^2 - m^2}{q^2} q^\mu F_0(q^2), \quad (15)$$

$$\langle \psi(2S)(P_2) | \bar{c} \gamma^\mu b | B_c(P_1) \rangle = \frac{2iV(q^2)}{M + m} \epsilon^{\mu\nu\rho\sigma} \epsilon_\nu^* P_{2\rho} P_{1\sigma}, \quad (16)$$

$$\begin{aligned} \langle \psi(2S)(P_2) | \bar{c} \gamma^\mu \gamma_5 b | B_c(P_1) \rangle &= 2mA_0(q^2) \frac{\epsilon^* \cdot q}{q^2} q^\mu + (M + m)A_1(q^2) \left[ \epsilon^{*\mu} - \frac{\epsilon^* \cdot q}{q^2} q^\mu \right] \\ &\quad - A_2(q^2) \frac{\epsilon^* \cdot q}{M + m} \left[ (P_1 + P_2)^\mu - \frac{M^2 - m^2}{q^2} q^\mu \right], \end{aligned} \quad (17)$$

where  $q = P_1 - P_2$  is the momentum transfer and  $P_1(P_2)$  is the momentum of the initial (final) state meson.  $M$  is the mass of  $B_c$  meson, and  $\epsilon^*$  is the polarization vector of  $\psi(2S)$  meson. In the large-recoil limit, say  $q^2 = 0$ , we have

$$F_0(0) = F_+(0), \quad A_0(0) = \frac{1+r}{2r} A_1(0) - \frac{1-r}{2r} A_2(0). \quad (18)$$

It is straightforward to calculate the form factors  $F_0(q^2)$ ,  $V(q^2)$  and  $A_{0,1}(q^2)$  at the tree level in the pQCD. They read as

$$\begin{aligned}
F_0 &= 2\sqrt{\frac{2}{3}}\pi M^2 f_B C_f \int_0^1 dx_2 \int_0^\infty b_1 b_2 db_1 db_2 \exp\left(-\frac{\omega_B^2 b_1^2}{2}\right) \\
&\times \left\{ [\psi^v(x_2, b_2)(x_2 - 2r_b) - \psi^s(x_2, b_2)r(2x_2 - r_b)] E_{ab}(t_a) h(\alpha_e, \beta_a, b_1, b_2) S_t(x_2) \right. \\
&+ \left. [\psi^v(x_2, b_2)(r_c + r^2(1 - x_1)) - \psi^s(x_2, b_2)2r(1 - x_1 + r_c)] E_{ab}(t_b) h(\alpha_e, \beta_b, b_2, b_1) S_t(x_1) \right\}, \quad (19)
\end{aligned}$$

$$\begin{aligned}
V &= 2\sqrt{\frac{2}{3}}(1+r)\pi M^2 f_B C_f \int_0^1 dx_2 \int_0^\infty b_1 b_2 db_1 db_2 \exp\left(-\frac{\omega_B^2 b_1^2}{2}\right) \\
&\times \left\{ [\psi^V(x_2, b_2)r(1 - x_2) + \psi^T(x_2, b_2)(r_b - 2)] E_{ab}(t_a) h(\alpha_e, \beta_a, b_1, b_2) S_t(x_2) \right. \\
&- \left. \psi^V(x_2, b_2)r E_{ab}(t_b) h(\alpha_e, \beta_b, b_2, b_1) S_t(x_1) \right\}, \quad (20)
\end{aligned}$$

$$\begin{aligned}
A_0 &= 2\sqrt{\frac{2}{3}}\pi M^2 f_B C_f \int_0^1 dx_2 \int_0^\infty b_1 b_2 db_1 db_2 \exp\left(-\frac{\omega_B^2 b_1^2}{2}\right) \\
&\times \left\{ [\psi^L(x_2, b_2)(x_2 - 2r_b) - \psi^t(x_2, b_2)r(2x_2 - r_b)] E_{ab}(t_a) h(\alpha_e, \beta_a, b_1, b_2) S_t(x_2) \right. \\
&- \left. \psi^L(x_2, b_2)[r_c + r^2(1 - x_1)] E_{ab}(t_b) h(\alpha_e, \beta_b, b_2, b_1) S_t(x_1) \right\}, \quad (21)
\end{aligned}$$

$$\begin{aligned}
A_1 &= 2\sqrt{\frac{2}{3}}\frac{r}{1+r}\pi M^2 f_B C_f \int_0^1 dx_2 \int_0^\infty b_1 b_2 db_1 db_2 \exp\left(-\frac{\omega_B^2 b_1^2}{2}\right) \\
&\times \left\{ [\psi^V(x_2, b_2)(1 + x_2 - r^2(1 - x_2) - 4r_b) + \psi^T(x_2, b_2)\left[r(2 - 4x_2 + r_b) + \frac{r_b - 2}{r}\right]] \right. \\
&\times \left. E_{ab}(t_a) h(\alpha_e, \beta_a, b_1, b_2) S_t(x_2) - \psi^V(x_2, b_2)[1 - x_1 + 2r_c + r^2] E_{ab}(t_b) h(\alpha_e, \beta_b, b_2, b_1) S_t(x_1) \right\}, \quad (22)
\end{aligned}$$

with  $r = \frac{m}{M}$  and  $r_{b,c} = \frac{m_{b,c}}{M}$ . The functions  $E_{ab}$ , the scales  $t_{a,b}$  and the hard functions  $h$  are given in Appendix B of the Ref. [29].

The quark-diagrams contribute to the  $B_c \rightarrow \psi(2S)\pi, \eta_c(2S)\pi$  decays are displayed in Fig. 3, where (a) and (b) are factorizable topology, (c) and (d) are nonfactorizable topology. The effective Hamiltonian relevant to the considered decays is written as [40]

$$\mathcal{H}_{eff} = \frac{G_F}{\sqrt{2}} V_{cb}^* V_{ud} [C_1(\mu) O_1(\mu) + C_2(\mu) O_2(\mu)] + \text{h.c.}, \quad (23)$$

with  $V_{cb}^*$  and  $V_{ud}$  the Cabibbo-Kobayashi-Maskawa (CKM) matrix elements,  $C_{1,2}(\mu)$  the Wilson coefficients, and  $O_{1,2}(\mu)$  the effective four quark operators

$$\begin{aligned}
O_1(\mu) &= \bar{b}_\alpha \gamma^\mu (1 - \gamma_5) c_\beta \otimes \bar{u}_\beta \gamma_\mu (1 - \gamma_5) d_\alpha, \\
O_2(\mu) &= \bar{b}_\alpha \gamma^\mu (1 - \gamma_5) c_\alpha \otimes \bar{u}_\beta \gamma_\mu (1 - \gamma_5) d_\beta,
\end{aligned} \quad (24)$$

where  $\alpha$  and  $\beta$  are the color indices. Since the four quarks in the operators are different from each other, there is no penguin contribution. Therefore there will be no  $CP$  violation in the decays of  $B_c \rightarrow \psi(2S)\pi, \eta_c(2S)\pi$  within standard model. After a straightforward calculation using the pQCD formalism of Eq. (2), we have the decay amplitudes

$$\mathcal{A}(B_c \rightarrow (\psi(2S), \eta_c(2S))\pi) = V_{cb}^* V_{ud} [(C_2 + \frac{1}{3}C_1)\mathcal{F}_e + C_1\mathcal{M}_e]. \quad (25)$$

The detailed expressions of  $\mathcal{F}_e$  and  $\mathcal{M}_e$  are the same as  $B_c \rightarrow (J/\psi, \eta_c)\pi$  decay modes in Appendix (A) of the Ref. [29], except the replacements  $J/\psi \rightarrow \psi(2S)$  and  $\eta_c \rightarrow \eta_c(2S)$ .

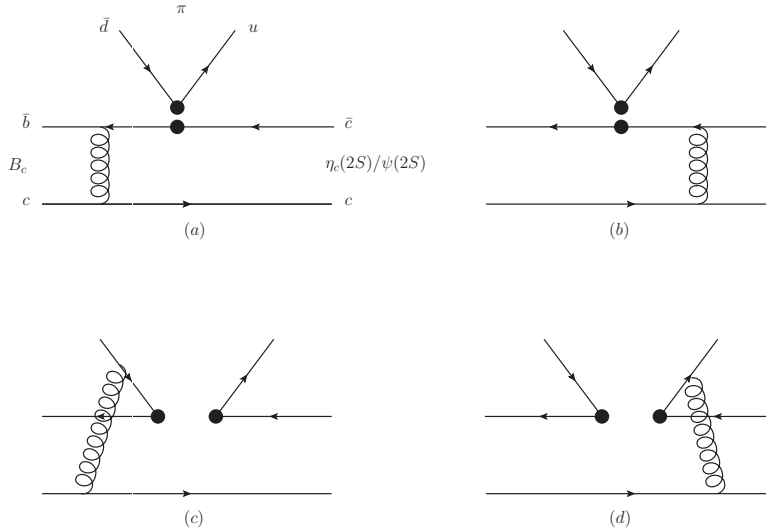


FIG. 3: Feynman diagrams for  $B_c \rightarrow \psi(2S)\pi, \eta_c(2S)\pi$  decays.

#### IV. NUMERICAL RESULTS AND DISCUSSIONS

In the numerical calculations we need the following input parameters (in units of GeV) [41]:

$$m_c = 1.275, \quad m_b = 4.18, \quad M_{B_c} = 6.277, \quad m_{\psi(2S)} = 3.686, \quad m_{\eta_c(2S)} = 3.639. \quad (26)$$

For relevant CKM matrix elements we use  $V_{cb} = (40.9 \pm 1.1) \times 10^{-3}$  and  $V_{ud} = 0.97425 \pm 0.00022$  [41].

The decay constant  $f_{\psi(2S)}$  can be derived from the process  $\psi(2S) \rightarrow e^+e^-$  by the relationship

$$f_{\psi(2S)} = \sqrt{\frac{3m_{\psi(2S)}\Gamma_{\psi(2S) \rightarrow e^+e^-}}{4\pi\alpha^2 Q_c^2}}, \quad (27)$$

using the data given in [41]

$$\Gamma_{\psi(2S) \rightarrow e^+e^-} = (2.36 \pm 0.04) \text{ keV}. \quad (28)$$

Then we have  $f_{\psi(2S)} = 296_{-2}^{+3}$  MeV. The decay constant  $f_{\eta_c(2S)}$  can be determined by the double photons decay of  $\eta_c(2S)$  as

$$f_{\eta_c(2S)} = \sqrt{\frac{81\pi m_{\eta_c(2S)}\Gamma_{\eta_c(2S) \rightarrow \gamma\gamma}}{4(4\pi\alpha)^2}}. \quad (29)$$

Using the measured results of the branching fractions  $\eta_c(2S) \rightarrow \gamma\gamma$  and the full width of  $\eta_c(2S)$  [41],

$$\mathcal{B}(\eta_c(2S) \rightarrow \gamma\gamma) = (1.9 \pm 1.3) \times 10^{-4}, \quad \Gamma_{\eta_c(2S)} = 11.3_{-2.9}^{+3.2} \text{ MeV}, \quad (30)$$

we can get the decay constant  $f_{\eta_c(2S)} = 243_{-111}^{+79}$  MeV. As for the decay constant for  $B_c$ , we adopt  $f_{B_c} = 489$  MeV [42].

Our numerical results for the form factors  $F_0^{B_c \rightarrow \eta_c(2S)}$ ,  $A_{0,1,2}^{B_c \rightarrow \psi(2S)}$  and  $V^{B_c \rightarrow \psi(2S)}$  are listed in Table I. We find that the form factors are close by different approaches within errors, except the results in Ref. [11] which is typically smaller. Some dominant uncertainties are considered in our numerical values: the first error comes from the shape parameters  $\omega_B = 0.6 \pm 0.1$  ( $\omega = 0.2 \pm 0.1$ ) GeV for the  $B_c(\psi(2S)/\eta_c(2S))$  meson, the second one is induced by  $m_c = 1.275 \pm 0.025$  GeV, the third error comes from the decay constants of the  $\psi(2S)$  or  $\eta_c(2S)$  meson, and the last one is caused by the variation of the hard scale from  $0.75t$  to  $1.25t$  in the Eq. (2), which characterize the size of next-to-leading order contribution. It is found that the main errors come from the uncertainties of the shape parameters and the charm-quark mass. Therefore, the decay of  $B_c \rightarrow \psi(2S)(\eta_c(2S))$  provide a good platform to understand the wave function of the radially excited charmonium states and the constituent quark model. The uncertainty from the

TABLE I: The form factors for  $F_0^{B_c \rightarrow \eta_c(2S)}$ ,  $A_{0,1,2}^{B_c \rightarrow \psi(2S)}$  and  $V^{B_c \rightarrow \psi(2S)}$  at  $q^2 = 0$  evaluated by pQCD and by other methods in the literature. We also show theoretical uncertainties induced by the shape parameters,  $m_c$ ,  $f_{\psi(2s)}$  or  $f_{\eta_c(2s)}$  and the hard scale  $t$ , respectively.

	This work	Ref.[9]	Ref.[10] <sup>a</sup>	Ref.[11]	Ref.[43]
$F_0$	$0.70^{+0.09+0.12+0.23+0.02}_{-0.05-0.10-0.32-0.01}$	–	0.325	0.27	–
$A_0$	$0.56^{+0.09+0.07+0.00+0.01}_{-0.05-0.04-0.00-0.01}$	0.45	0.42	0.23	0.20
$A_1$	$0.56^{+0.13+0.06+0.00+0.01}_{-0.04-0.03-0.00-0.01}$	0.335	0.35	0.18	0.38
$A_2$	$0.62^{+0.27+0.04+0.01+0.02}_{-0.05-0.01-0.01-0.00}$	0.102	0.15	0.14	0.90
$V_0$	$0.95^{+0.18+0.15+0.01+0.03}_{-0.08-0.10-0.01-0.01}$	0.525	0.73	0.24	0.90

<sup>a</sup>Comparing the definitions of the transition form factor of Ref. [10] with ours, we have the following relations at the maximal recoil point,

$$\begin{aligned}
 F_0 &= f^+, \quad V = (M+m)g, \quad A_1 = \frac{f}{M+m}, \quad A_2 = -(M+m)a_+, \\
 A_0 &= \frac{f + (M^2 - m^2)a_+ + q^2 a_-}{2m},
 \end{aligned} \tag{31}$$

where the values of  $f^+$ ,  $g$ ,  $f$ ,  $a_+$ ,  $a_-$  are given in [10].

TABLE II: Branching ratios ( $10^{-4}$ ) of the  $B_c \rightarrow \eta_c(2S)\pi, \psi(2S)\pi$  decays. The errors induced by the same sources as they in TABLE I.

Modes	This work	[9] <sup>a</sup>	[10]	[11]	[12]	[13]	[14]	[15]	[44] <sup>b</sup>
$B_c \rightarrow \eta_c(2S)\pi$	$10.3^{+3.4+4.0+7.8+1.2}_{-1.8-2.8-7.2-0.4}$	–	2.4	1.7	2.2	2.4	0.66	2.87	–
$B_c \rightarrow \psi(2S)\pi$	$6.7^{+2.8+1.8+0.1+0.7}_{-1.1-1.2-0.1-0.3}$	2.97	3.7	1.1	0.63	2.2	2.0	2.66	7.6(5.8)

<sup>a</sup>We quote the result with the modified wave functions for  $\psi(2S)$ .

<sup>b</sup>The nonbracketed (bracketed) results are evaluated at the NLO (LO) level.

decay constant of  $\eta_c(2S)$  meson is large due to the low accuracy measurement of the branching fraction in Eq. (30), the relevant uncertainty of  $F_0$  is large, too. We expect that it could be measured precisely at LHCb and Super-B factories in the near future. We also noticed that the error from the uncertainty of the hard scale  $t$  is small, which means the next-to-leading order contributions can be safely neglected. The errors from the uncertainty of the CKM matrix elements are very small, which have been neglected.

The branching fractions for the  $B_c \rightarrow \eta_c(2S)\pi, \psi(2S)\pi$  decays in the  $B_c$  meson rest frame can be written as

$$\mathcal{B}(B_c \rightarrow (\psi(2S), \eta_c(2S))\pi) = \frac{G_F^2 \tau_{B_c}}{32\pi M_B} (1 - r^2) |\mathcal{A}|^2, \tag{32}$$

where the decay amplitudes  $\mathcal{A}$  have been given explicitly in Eq. (25). In Table II, we show the results of the branching fractions for the two-body nonleptonic  $B_c \rightarrow \eta_c(2S)\pi, \psi(2S)\pi$  decays, where the sources of the errors in the numerical estimates have the same origin as in the discussion of the form factors in Table I. It is easy to see that the most important theoretical uncertainty are caused by the nonperturbative shape parameters, the charm-quark mass and the decay constant  $f_{\eta_c(2S)}$ , which can be improved by future experiments. It is found that the branching fractions of  $B_c$  decays to the 2S state are smaller than those of 1S state in our previous study [29] in the perturbative QCD approach. This phenomenon can be understood from the wave functions of the two states. The presence of the node in the 2S wave function, which can be seen in Fig. 1, causes the overlap between the initial and final state wave functions becomes smaller. Besides, the tighter phase space and the smaller decay constants of 2S state also suppress their branching ratios.

We also make a comparison of our results with the previous studies. One can see that our results are comparable to those of [44] within the error bars, but larger than the results from other modes. This is because that they have used the smaller form factors at maximum recoil. Regardless of this effect, our results are consistent with theirs. For example, as shown in Tables I and II, our values of  $A_0$  and  $F_0$  are about 2.5 times the results of Ref. [11], and result in our branching ratios are 6 times larger than theirs. For a more direct comparison with the available experimental data, we compare the present results in Table II with those for the decays of  $B_c$  to S-wave charmonium states  $J/\psi$  and  $\eta_c$  (also based on the harmonic-oscillator wave functions), whose results can be found in Ref.[29], and obtain the ratios  $\mathcal{B}(B_c \rightarrow (\psi(2S)\pi))/\mathcal{B}(B_c \rightarrow (J/\psi)\pi) = 0.29^{+0.17}_{-0.11}$  and  $\mathcal{B}(B_c \rightarrow (\eta_c(2S)\pi))/\mathcal{B}(B_c \rightarrow (\eta_c\pi)) = 0.35^{+0.36}_{-0.29}$ . The former is

TABLE III: The values of decay amplitude from twist-2 and twist-3 charmonium wave functions for  $B_c \rightarrow \eta_c(2S)\pi, \psi(2S)\pi$  decays. The results are given in units of  $\text{GeV}^3$ .

Modes	twist-2	twist-3	total
$\mathcal{A}(B_c \rightarrow \psi(2S)\pi)$	-1.7-0.07i	-0.4-0.06i	-2.1-0.13i
$\mathcal{A}(B_c \rightarrow \eta_c(2S)\pi)$	-1.5-2.3i	3.9+1.4i	2.4+0.9i

consistent with the data  $0.25 \pm 0.068 \pm 0.014$  [8], and also comparable with the recent prediction of the Bethe-Salpeter relativistic quark model [15], 0.24. This fact may indicate that the harmonic oscillator wave functions for radially excited states are reasonable and applicable. Although the  $B_c \rightarrow \eta_c(2S)\pi$  decay have not been yet measured so far, the predicted large branching ratio ( $10^{-3}$ ) makes it possible to be measured soon at LHCb experiment or future facility.

We now investigate the relative importance of the twist-2 and twist-3 contributions in Eq. (4) to the decay amplitude, whose results are displayed separately in Table III, where the label “twist-2 (twist-3)” corresponding to the contribution of the twist-2 (twist-3) distribution amplitude only, while the “total” corresponding to the contributions both of them. It is found that the contribution of twist-3 distribution amplitude is not power-suppressed for  $B_c \rightarrow \eta_c(2S)\pi$  decay, whose contribution is 1.5 times larger than the contribution of twist-2. The reason is that the term  $\psi^s(x_2, b_2)2r$  in Eq. (19) from Fig. 3-b give the dominant contribution to the decay amplitude, since the asymptotic model of twist-3 distribution amplitude in Eq. (13) for  $\eta_c(2S)$  meson have no factor like  $x(1-x)$  to suppress its integral value in the end-point region which lead to large enhancement compared with twist-2 contribution. However, because twist-3 terms of the  $\psi(2S)$  meson distribution amplitude do not contribute to the  $B_c \rightarrow \psi(2S)\pi$  decay amplitude from Fig.3-(b), the contribution from other diagrams with twist-3 distribution amplitude is only one-fifth smaller than that of twist-2 contribution in this process. It is also find that there is very strong interference between contributions of twist-2 and twist-3 wave functions for both  $B_c \rightarrow \psi(2S)\pi$  and  $B_c \rightarrow \eta_c(2S)\pi$  decays. The numerical results show that the contributions from twist-3 wave function have an opposite sign between the two channels. This results in a constructive interference for the former, but a destructive interference for the latter. The reason is that the amplitudes are different between the two decays at twist-3 level, which can be seen in Eqs. (A1) and (A4) of [29]. The similar situation also exists in  $B_c \rightarrow D\pi, D^*\pi$  [26] decays.

## V. CONCLUSION

We calculated the form factors of the weak  $B_c$  decays to radially excited charmonia and the branching ratios of  $B_c \rightarrow \psi(2S)\pi, \eta_c(2S)\pi$  decays in the pQCD approach. The new charmonium distribution amplitudes based on the radial Schrödinger wave function of  $n=2, l=0$  state for the harmonic oscillator potential are employed. We discussed theoretical uncertainties arising from the nonperturbative shape parameters, the charm-quark mass, the decay constants and the scale dependence. It is found that the main uncertainties of the concerned processes come from the shape parameters and the charm-quark mass. The theoretically evaluated ratios  $\mathcal{B}(B_c \rightarrow (\psi(2S)\pi))/\mathcal{B}(B_c \rightarrow (J/\psi\pi)) = 0.29_{-0.11}^{+0.17}$  is consistent with the data, which indicate the harmonic-oscillator wave functions works well not only for the ground state charmonium, but also for the radially excited charmonia. It is also found that the twist-3 charmonium distribution amplitude gives a large contribution, especially for  $B_c \rightarrow \eta_c(2S)\pi$  decay, whose branching fraction is at the order of  $10^{-3}$ , which could be tested at the ongoing large hadron collider.

## Acknowledgments

This work is supported in part by National Natural Science Foundation of China under Grants No. 11235005, No. 11347168, 11375208 and No. 11405043, by Natural Science Foundation of Hebei Province of China under Grant No. A2014209308 and by China Postdoctoral Science Foundation.

- 
- [1] Y.N. Gao *et al.*, Chin. Phys. Lett. **27**, 061302 (2010).
  - [2] R. Aaij *et al.* [LHCb Collaboration], Phys. Rev. Lett. **108**, 251802(2012).
  - [3] R. Aaij *et al.* [LHCb Collaboration], JHEP **09**, 075 (2013).



- [4] R. Aaij *et al.* [LHCb Collaboration], Phys. Rev. D **87**, 112012 (2013).
- [5] R. Aaij *et al.* [LHCb Collaboration], JHEP **11**, 094 (2013).
- [6] R. Aaij *et al.* [LHCb Collaboration], Phys. Rev. Lett. **111**, 181801 (2013).
- [7] G. Aad *et al.* [ATLAS Collaboration], Phys. Rev. Lett. **113**, 212004 (2014).
- [8] R. Aaij *et al.* [LHCb Collaboration], Phys. Rev. D **87**, 071103 (2013).
- [9] H.W. Ke, T. Liu and X.Q. Li, Phys. Rev. D **89**, 017501 (2014).
- [10] I. Bediaga and J. H. Muñoz, arXiv:1102.2190.
- [11] R.N. Faustov and V.O. Galkin, Phys. Rev. D **68**, 094020 (2003).
- [12] J.F. Liu and K.T. Chao, Phys. Rev. D **56**, 4133 (1997).
- [13] C.H. Chang and Y.Q. Chen, Phys. Rev. D **49**, 3399 (1994).
- [14] P. Colangelo and F. De Fazio, Phys. Rev. D **61**, 034012 (2000).
- [15] C.H. Chang, H.F. Fu, G.L. Wang and J.M. Zhang, arXiv:1411.3428.
- [16] Y.Y. Keum, H.-n. Li, and A.I. Sanda, Phys. Lett. B **504**, 6 (2001); Phys. Rev. D **63**, 054008 (2001); C. -D. Lü, K. Ukai and M. -Z. Yang, Phys. Rev. D **63**, 074009 (2001); C. -D. Lü and M. -Z. Yang, Eur. Phys. J. C **23**, 275 (2002).
- [17] X. Liu, Z.J. Xiao and C.D. Lü, Phys. Rev. D **81**, 014022 (2010).
- [18] X. Liu and Z.J. Xiao, Phys. Rev. D **81**, 074017 (2010).
- [19] Y. Yang, J. Sun and N. Wang, Phys. Rev. D **81**, 074012 (2010).
- [20] X. Liu and Z.J. Xiao, Phys. Rev. D **82**, 054029 (2010).
- [21] X. Liu and Z.J. Xiao, J. Phys. G **38**, 035009 (2011).
- [22] Z.J. Xiao and X. Liu, Phys. Rev. D **84**, 074033 (2011).
- [23] Z.J. Xiao and X. Liu, Chin. Sci. Bull. **59**, 3748 (2014).
- [24] J.F. Cheng, D.S. Du and C.D. Lü, Eur. Phys. J. C **45**, 711 (2006).
- [25] J. Zhang and X.Q. Yu, Eur. Phys. J. C **63**, 435 (2009).
- [26] R. Zhou and Z.T. Zou, and C.D. Lü, Phys. Rev. D **86**, 074008 (2012).
- [27] R. Zhou and Z.T. Zou, and C.D. Lü, Phys. Rev. D **86**, 074019 (2012).
- [28] Z.T. Zou, X. Yu and C.D. Lü, Phys. Rev. D **87**, 074027 (2013).
- [29] R. Zhou and Z.T. Zou, Phys. Rev. D **90**, 114030 (2014).
- [30] W.F. Wang, X. Yu, C.D. Lü, and Z.J. Xiao, Phys. Rev. D **90**, 094018 (2014).
- [31] P. Ball, JHEP **09**, 005 (1998); JHEP **01**, 010 (1999).
- [32] P. Ball and R. Zwicky, Phys. Rev. D **71**, 014015 (2005); P. Ball, V.M. Braun, and A. Lenz, JHEP **05**, 004 (2006).
- [33] J.F. Sun, D.S. Du and Y. Yang, Eur. Phys. J. C **60**, 107 (2009).
- [34] X.Q. Yu, and X.L. Zhou, Phys. Rev. D **81**, 037501 (2010).
- [35] J.F. Sun, Y.L. Yang, Q. Chang and G.R. Lu, Phys. Rev. D **89**, 114019 (2014).
- [36] C.H. Chang and H.-n. Li, Phys. Rev. D **71**, 114008 (2005).
- [37] A. E. Bondar and V. L. Chernyak, Phys. Lett. B **612**, 215 (2005).
- [38] W.F. Wang, Y.Y. Fan and Z.J. Xiao, Chin. Phys. C **37**, 093102 (2013).
- [39] C.F. Qiao and R.L. Zhu, Phys. Rev. D **87**, 014009 (2013).
- [40] G. Buchalla, A.J. Buras, M.E. Lautenbacher, Rev. Mod. Phys. **68**, 1125 (1996).
- [41] K.A. Olive *et al.* (Particle Data Group), Chin. Phys. C **38**, 090001 (2014).
- [42] T.W. Chiu, T. H. Hsieh, C. H. Huang, and K. Ogawa (TWQCD Collaboration), Phys. Lett. B **651**, 171 (2007).
- [43] Y.M. Wang and C.D. Lü, Phys. Rev. D **77**, 054003 (2008).
- [44] C.F. Qiao, P. Sun, D.S. Yang and R.L. Zhu, Phys. Rev. D **89**, 034008 (2014).